Exciton quenching at PEDOT:PSS anode in polymer blue-light-emitting diodes

D. Abbaszadeh, G. A. H. Wetzelaer, H. T. Nicolai, and P. W. M. Blom

Articles you may be interested in

Predictive modeling of the current density and radiative recombination in blue polymer-based light-emitting diodes
J. Appl. Phys. **109**, 064502 (2011); 10.1063/1.3553412

Triarylamine siloxane anode functionalization/hole injection layers in high efficiency/high luminance small-molecule green- and blue-emitting organic light-emitting diodes
J. Appl. Phys. **101**, 093101 (2007); 10.1063/1.2719276

Exciton quenching in poly(phenylene vinylene) polymer light-emitting diodes
Appl. Phys. Lett. **87**, 233511 (2005); 10.1063/1.2139622

Delayed recombination of detrapped space-charge carriers in poly[2-methoxy-5-(2 ′ -ethyl-hexyloxy)-1,4-phenylene vinylene]-based light-emitting diode
J. Appl. Phys. **97**, 114505 (2005); 10.1063/1.1914949

Recombination kinetics in wide gap electroluminescent conjugated polymers with on-chain emissive defects
J. Appl. Phys. **93**, 5973 (2003); 10.1063/1.1566091

Exciton quenching at PEDOT:PSS anode in polymer blue-light-emitting diodes

D. Abbaszadeh,[1,2] G. A. H. Wetzelaer,[1,2] H. T. Nicolai,[3] and P. W. M. Blom[4,5,a]

[1]*Molecular Electronics, Zernike Institute for Advanced Materials, University of Groningen, Nijenborgh 4, 9747 AG, Groningen, The Netherlands*
[2]*Dutch Polymer Institute, P.O. Box 902, 5600 AX, Eindhoven, The Netherlands*
[3]*TNO/Holst Centre, High Tech Campus 31, 5605 KN, Eindhoven, The Netherlands*
[4]*Max Planck Institute for Polymer Research, Ackermannweg 10, 55128 Mainz, Germany*
[5]*Department of Physics, Faculty of Science, King Abdulaziz University, Jeddah, Saudi Arabia*

The quenching of excitons at the poly(3,4-ethylenedioxythiophene):poly(styrenesulfonic acid) (PEDOT:PSS) anode in blue polyalkoxyspirobifluorene-arylamine polymer light-emitting diodes is investigated. Due to the combination of a higher electron mobility and the presence of electron traps, the recombination zone shifts from the cathode to the anode with increasing voltage. The exciton quenching at the anode at higher voltages leads to an efficiency roll-off. The voltage dependence of the luminous efficiency is reproduced by a drift-diffusion model under the condition that quenching of excitons at the PEDOT:PSS anode and metallic cathode is of equal strength. Experimentally, the efficiency roll-off at high voltages due to anode quenching is eliminated by the use of an electron-blocking layer between the anode and the light-emitting polymer. © 2014 AIP Publishing LLC. [http://dx.doi.org/10.1063/1.4903952]

I. INTRODUCTION

Organic electronics based on semiconducting polymers have garnered significant attention because of a number of advantages, including potentially cost-effective solution processability and flexibility of the final product. An attractive example of a device based on conjugated polymers is the polymer light-emitting diode (PLED). To fabricate a PLED with optimal performance, it is crucial to understand the physical processes that govern device operation. These processes include the injection, transport, and recombination (radiative and nonradiative) of charge carriers, as well as exciton quenching and surface recombination at the electrodes.[1] It was shown that the hole transport in many conjugated polymers shows trap-free behavior, while electron transport is strongly limited by the presence of electron traps. For a range of conjugated polymers, these electron traps were observed to be situated at an energy of ~3.6 eV below the vacuum level with a typical density of ~ 3–$5 \times 10^{23}\,\mathrm{m}^{-3}$.[2] The apparently universally present electron traps not only limit the electron transport but the trapped electrons also recombine with free holes via a nonradiative trap-assisted recombination process, which competes with the emissive bimolecular Langevin recombination.[1] A direct consequence of the trap-limited electron transport is that the exciton recombination zone is situated near the cathode in a PLED. The excitons formed near the metallic cathode are quenched by the metallic electrode, thereby reducing the efficiency. With increasing voltage, the electron traps are gradually filled and the excitons are generated more homogeneously in the active layer, leading to an increase of the efficiency with

voltage. In the first PLED device models, this increase of efficiency with voltage was used to estimate the width of the cathode quenching (CQ) region. A width of approximately 10 nm was found.[3] Using time-resolved photoluminescence, it was observed that the quenching by direct radiationless energy transfer to the metal is further enhanced by diffusion of excitons into the depletion area of the exciton population at the polymer/metal interface.[4] For an aluminum electrode on a layer of poly(*p*-phenylene vinylene) derivative, it was found that strong exciton quenching occurs within a region of about 15 nm, which can be decomposed in a characteristic energy-transfer range x_0 of 7.5 nm and an exciton diffusion length L_D of 6 nm.

In contrast to cathode quenching, the role of anode quenching in PLEDs is less clear, since in many PLEDs, the recombination zone is situated in the vicinity of the cathode due to the trap-limited electron transport. In addition, there exists a controversy about whether or not the doped conductive polymer poly(3,4-ethylenedioxythiophene):poly(styrenesulfonic acid) (PEDOT:PSS), which often serves as a hole-injection layer in PLEDs, efficiently quenches excitons that are formed near the anode. Lee *et al.* studied both graphene oxide and PEDOT:PSS as hole-injection layers and concluded that PEDOT:PSS is a highly quenching anode.[5] Kim *et al.* and Yim *et al.* showed that severe luminescence quenching occurs near the interface between PEDOT:PSS and the polymer poly(9,9′-di-*n*-octylfluorene-*alt*-benzothiadiazole) (F8BT).[6,7] This issue could be overcome by insertion of an electron- (and exciton-) blocking layer between PEDOT:PSS and the emissive layer. Such a layer is frequently applied to fabricate efficient PLEDs.[14,19,20] Contrary to these findings, Köhnen *et al.* observed a strong yellow emission for a very thin layer (<1 nm) of cross-linked poly(*p*-phenylene vinylene) derivative Super Yellow on top

---

[a]Author to whom correspondence should be addressed. Electronic mail: blom@mpip-mainz.mpg.de.

of PEDOT:PSS, subsequently coated by an 80 nm layer of blue-emitting polymer.[8]

To investigate the influence of anode quenching in an operating PLED, it is necessary that excitons are formed near the anode. A necessary requirement for this is that the electron transport is superior to the hole transport. It has been reported that the electron mobility in an efficient blue-emitting polyalkoxyspirobifluorene copolymerized with N,N,N',N'-tetraaryldiamino biphenyl (PSF-TAD, shown in Fig. 1(a)) copolymer is at least an order of magnitude higher than the hole mobility.[9] Even though the mobility of free electrons is higher than the mobility of free holes, at low voltages, the electron transport is still limited by deep trapping sites, as usually found in conjugated polymers. However, at higher voltages, the electron transport becomes dominant due to filling of the traps with charge carriers. In a PLED, this results in a voltage-dependent position of the recombination zone, shifting from the cathode all the way to the anode with increasing bias voltage. Therefore, it is expected that anode quenching plays a role at higher voltages and light intensities.

Here, we investigate the influence of anode quenching in PSF-TAD PLEDs using numerical device simulations and compare the results with a reference polyalkoxyspirobifluorene (PSF) polymer where the charge transport is fully hole-dominated. Anode quenching is found to limit the efficiency of PSF-TAD PLEDs at high voltages. We find that the PEDOT:PSS anode quenches excitons as efficient as the metallic Ba/Al cathode. This loss mechanism is subsequently eliminated by using an additional electron blocking layer on the anode side.

II. EXPERIMENTAL

PLEDs and single-carrier devices were fabricated on glass substrates with a patterned indium-tin oxide (ITO) layer. The substrates were cleaned, dried, and treated with UV-ozone. The emissive polymer polyalkoxyspirobifluorene-N,N,N',N-tetraaryldiamino biphenyl (PSF-TAD) and optional poly(9-vinylcarbazole) (PVK, shown in Fig. 1(b)) electron-blocking layers were spin-coated in a nitrogen atmosphere from toluene and chlorobenzene solutions, respectively. To measure the electron transport, the polymer layer was sandwiched between thermally evaporated Al (30 nm) and Ba/Al (5/100 nm) contacts on a glass substrate, resulting in an electron-only device. For measuring the hole transport, hole-only devices were fabricated in which the

polymer layer was sandwiched between ITO/PEDOT:PSS (Clevios™ P VP AI 4083) and MoO_3/Al electrodes, which both have sufficiently high work functions for Ohmic hole injection, while blocking the injection of electrons. For double-carrier devices, ITO/PEDOT:PSS was used as the anode and Ba/Al as the cathode.

III. RESULTS AND DISCUSSION

To analyze the effect of anode quenching in PLEDs, we first investigate the electron and hole transport. Therefore, electron- and hole-only devices have been prepared with PSF and PSF-TAD. The current density-voltage characteristics are shown in Figs. 2(a) and 2(b), respectively. For PSF, the electron current is lower than the hole current over the complete voltage range. By contrast, a crossover voltage is observed for PSF-TAD, above which the electron current is dominant. Since the intrinsic electron mobility of both polymers is similar the difference in the measured electron current originates from a different trap density. Modeling of the electron transport with a drift-diffusion model results in electron-trap densities of $3 \times 10^{23} \, m^{-3}$ and $1.3 \times 10^{23} \, m^{-3}$ for PSF and PSF-TAD, respectively, with a trap depth E_t of ~0.65 eV below the LUMO and a Gaussian distribution σ_t of ~0.1 eV.[10] The electron and hole mobility are described by the extended Gaussian disorder model (EGDM), which includes the effect of electric field and carrier density on the mobility.[1] Contrary to electron transport, hole transport can be described without additional charge trapping.

With the parameters for hole and electron transport known, the spatial distribution of the recombination zone in a PLED can be simulated, as shown in Figs. 2(c) and 2(d). Due to the more balanced transport in PSF-TAD as compared to PSF, the recombination zone is distributed across a significantly larger part of the layer thickness. Furthermore, it is observed that the recombination zone shifts more to the anode at higher voltages for PSF-TAD, whereas recombination remains near the cathode in PSF. Therefore, it is expected that anode quenching only plays a role in PSF-TAD at higher current densities and is virtually absent in PSF.

By including the loss mechanisms of cathode and anode quenching of excitons, next to the nonradiative trap-assisted recombination loss mechanism, the efficiency of the PLED as a function of driving voltage can be simulated.[10] Fig. 3 shows the experimental and simulated current efficiencies for PLEDs of different thicknesses. Fig. 3(a) shows the results for PSF, which has a higher trap density compared to
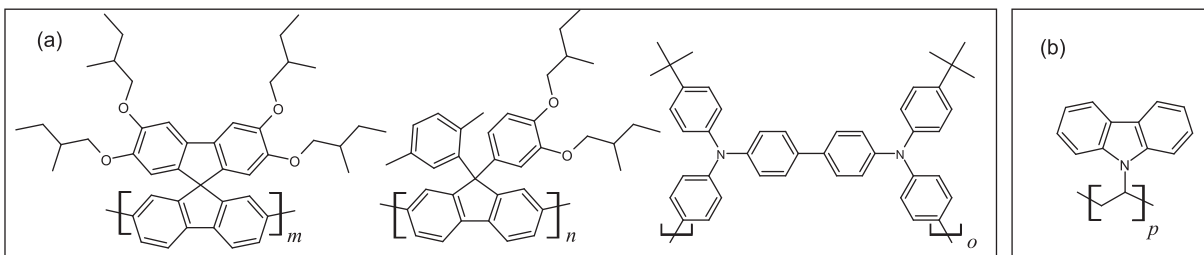

FIG. 1. (a) Chemical structure of the PSF host copolymer and the TAD hole transport unit. The composition of the PSF copolymer is m = 50% and n = 50%. In the PSF-TAD copolymer has a TAD concentration of 10%, resulting in a composition of m = 50%, n = 40%, and o = 10%. (b) Chemical structure of PVK.
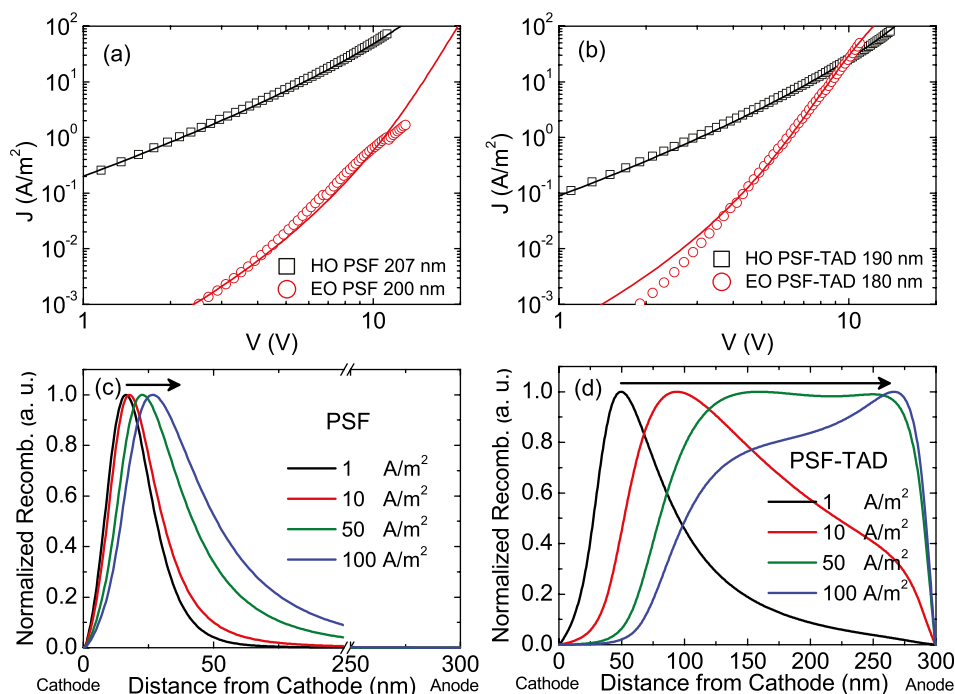
FIG. 2. (a) and (b) Experimental (symbols) and simulated (solid lines) current density-voltage characteristics of hole-only (HO) and electron-only (EO) devices for PSF (a) and PSF-TAD (b). (c) and (d) Normalized recombination profile (recombination rate vs distance from cathode) inside a simulated PLED (double-carrier) device of 300 nm for PSF with an electron-trap density of $3 \times 10^{23} \, \mathrm{m}^{-3}$ (c) and PSF-TAD with an electron-trap density of $1.3 \times 10^{23} \, \mathrm{m}^{-3}$ (d).

PSF-TAD [Fig. 3(b)]. For the PSF polymer, the efficiency initially increases with voltage in the low-voltage regime due to reduced nonradiative trap-assisted recombination losses and reduced cathode quenching. To model the cathode quenching, a one-dimensional exciton diffusion model is used with input parameters x_0 and L_D.[4] It has recently been observed that the electron traps are also responsible for the quenching of excitons in a range of conjugated polymers and small molecules.[11] As a result, the average exciton diffusion length L_D is equal to half of the distance between the electron traps. From the measured electron trap concentration of $3 \times 10^{23} \, \mathrm{m}^{-3}$, we find for PSF an exciton diffusion length of 6.3 nm. The only remaining parameter is x_0, the characteristic range of energy transfer toward the metal, which we determine to be 4 nm. For PSF, it makes no difference whether we take anode quenching into account or not, since the recombination takes place near the cathode over the complete voltage range.

The PSF-TAD polymer with a trap density of $1.3 \times 10^{23} \, \mathrm{m}^{-3}$ shows a markedly different behavior in the plot of efficiency vs. voltage. Due to the lower trap density in PSF-TAD compared to PSF, the amount of trap-assisted recombination and cathode quenching (due to enhanced

trap-filling) is reduced, resulting in a steeper slope in the efficiency-voltage plot. Moreover, a drop in efficiency is observed at higher voltages for PSF-TAD, which is not observed in PSF PLEDs. The shift of the efficiency maximum toward higher voltages with increasing layer thickness is a natural result of the lower electric fields (and current densities) in thicker films.

As a first step to model the efficiency of PSF-TAD PLEDs, we only take cathode quenching into account, as done for PSF. We again set x_0 equal to 4 nm, whereas the exciton diffusion length is increased to 11 nm due to the reduced electron trap density of $1.3 \times 10^{23} \, \mathrm{m}^{-3}$. As can be observed from the dashed lines in Fig. 3(b), the simulated efficiency curves consistently describe, without any additional parameter, the efficiency rise of the thick samples, where, in the voltage range considered, most of the excitons are still generated at the cathode. This shows that in both PSF and PSF-TAD PLEDs the cathode quenching is identical. However, for thinner devices, the model using only cathode quenching does not explain the efficiency of the PSF-TAD PLEDs. Therefore, as a next step, we also include quenching at the PEDOT:PSS anode, using the same quenching parameter x_0 of 4 nm, as also used for the metallic
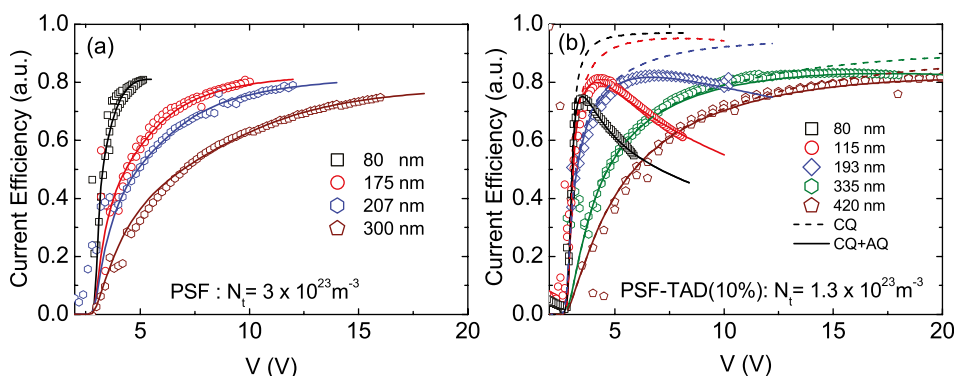

FIG. 3. Experimental (symbols) and simulated (lines) thickness-dependent current efficiency versus voltage for (a) the reference PSF polymer with a trap density of $3 \times 10^{23} \, \mathrm{m}^{-3}$, where only CQ is important, and (b) PSFTAD with a trap density of $1.3 \times 10^{23} \, \mathrm{m}^{-3}$. The solid lines represent simulations with equal quenching at both electrodes (CQ + AQ), whereas dashed lines represent the simulated current efficiency when only cathode quenching is introduced. (Experimental data were normalized to calculation).
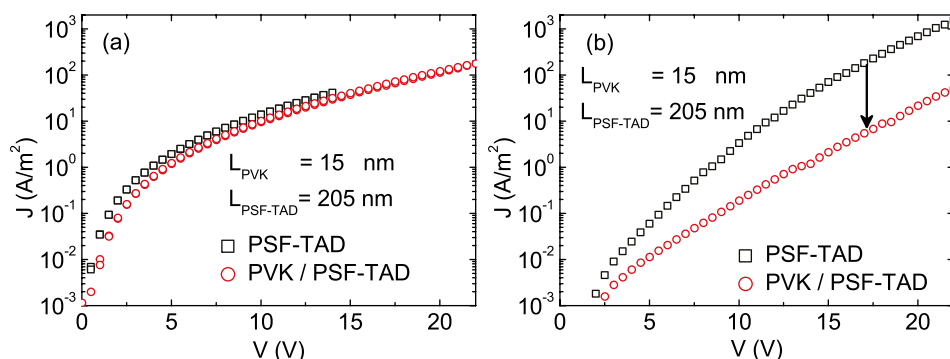
FIG. 4. (a) Hole and (b) electron currents of PSF-TAD single-layer (squares) and PVK/PSF-TAD bilayer (circles) hole- and electron-only devices. The thickness of the PVK and PSF-TAD layer amounted to 15 nm and 205 nm, respectively.

cathode. As shown by the solid lines in Fig. 3(b), taking into account identical exciton quenching for both electrodes, we can fully model the PLED device performance for all layer thicknesses.

From the numerical simulations, it is clear that the efficiency decrease at higher voltages can be attributed to exciton quenching at the anode. To confirm this model prediction, a further experimental validation is required. Fabrication of bilayer PLEDs with an additional electron blocking layer with proper energy levels should prevent excitons from being formed near the anode and also should prevent subsequent diffusion of the exciton toward the anode. If the efficiency roll-off at high voltages is indeed caused by anode quenching, this feature should be suppressed upon inclusion of an electron blocking layer. The use of a multilayer structure to confine charge recombination to the emitting layer and eliminate exciton quenching in order to improve OLED efficiency has been widely applied.[6,12–21] Fabricating a multilayer device with solution-processing techniques is complicated by the fact that deposition of a second layer will result in partial or complete dissolution of the previously deposited layer. To overcome this problem, researchers have proposed different techniques like cross linking the first layer(s),[12,13] using a liquid buffer layer,[14] using water-alcohol soluble materials,[15–17] and using orthogonal solvents, i.e., the solvent of the next layer should not dissolve the previous one.[18–21]

Here, we follow the orthogonal solvent approach by using an electron blocking layer based on the polymer PVK, which has a relatively low solubility. PVK is a well-known conducting polymer, which, when it has a high molecular weight, is not soluble in toluene, especially after the deposited layer is annealed at 150 °C. In addition, PVK has a very high LUMO (~ -2.2 eV for PVK[22] compared to ~ -2.6 eV for PSF[23]), which makes it suitable to use as an electron-blocking layer.

For the fabrication of these bilayer PLEDs, a 15 nm layer of high molecular weight PVK ($M_w \sim 1\,100\,000$, Sigma Aldrich) was spin coated on top of PEDOT:PSS and subsequently annealed at 150 °C. As a next step, a layer of PSF-TAD was spin coated on top of the PVK layer from toluene solution. To verify the influence of the PVK electron-blocking layer on the charge transport, hole-only and electron-only devices of such bilayer devices were fabricated. From Fig. 4(a), it appears that hole transport is not affected by the presence of the additional PVK layer. The small drop in hole current can be attributed to the slightly increased total thickness. The electron transport for single- and bilayers is shown in Fig. 4(b). For the electron-only devices, an Al bottom electrode is used to prevent hole injection, while the Ba/Al top electrode injects electrons into the PSF-TAD LUMO. The electron current is indeed blocked by the PVK layer, as evidenced by the reduction in current of more than an order of magnitude compared to the single-layer device. This shows that PVK should be effective in reducing anode quenching.

Fig. 5(a) shows the *J-V* characteristics for single and bilayer PLEDs. For the first scan up to 4.5 V, the bilayer device yields much lower currents compared to the single-layer device. After consecutive scans to higher voltages, it appears that around 4 V the current starts to increase sharply and light output is measured. A counter-clockwise hysteresis is observed, where the up scan follows the down scan of the previous measurement. Scanning to sufficiently high voltages (7–8 V in this case), results in saturation of the current and the hysteresis is no longer present in subsequent
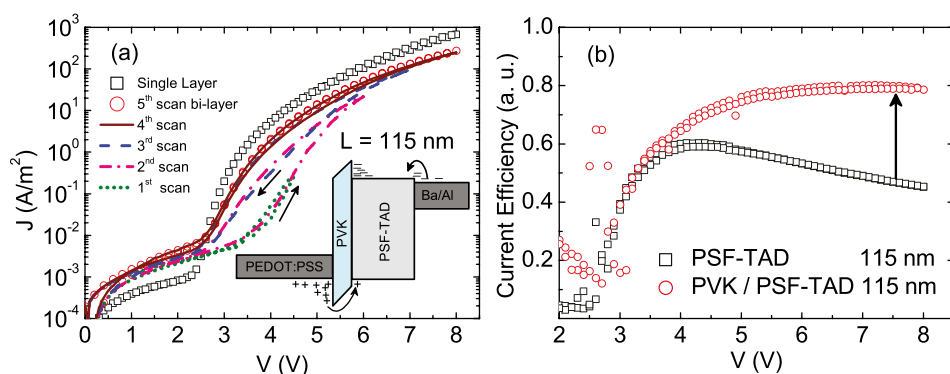

FIG. 5. (a) *J-V* characteristics of single-layer and bilayer PLEDs, showing 5 consecutive voltage scans for the bilayer device. (b) Efficiency versus voltage for single-layer and bilayer devices with equal thickness, the PVK layer thickness is $\sim$15 nm.

scans. The saturated current is only slightly lower than the current of the single-layer reference device. This effect is known as electron-enhanced hole injection, addressed by van Woudenbergh *et al.* for the PEDOT:PSS/PFO interface.[24] According to this effect, the accumulation or trapping of electrons at the interface between PVK and PSF-TAD enhances the hole injection from PEDOT:PSS into PVK and subsequently into the light-emitting polymer. Fig. 5(b) shows the current efficiency vs. voltage for the bilayer device, compared to a single-layer device with equal total layer thickness. We clearly observe that the efficiency roll-off at higher voltages, as observed in the single layer device, has disappeared. As predicted in the absence of anode quenching [dashed line Fig. 3(b)], the efficiency reaches a plateau value. This experimental result clearly proves that the decrease in efficiency at high voltages (and therefore high luminance) in PSF-TAD is due to anode quenching. The results show that implementing a suitable electron blocking layer eliminates energy transfer of the exciton into the anode.

IV. CONCLUSION

It was demonstrated that quenching of excitons at the PEDOT:PSS anode is responsible for the efficiency roll-off at higher voltages in blue-emitting PLEDs. This effect could be simulated with a numerical device model, which was able to reproduce the experimental results. The quenching of excitons at the polymeric anode and metallic cathode were observed to be equally efficient. The role of anode quenching was further validated through the application of an electron-blocking layer between the anode and the emitting layer. Application of a PVK blocking layer eliminated the efficiency roll-off at higher voltages, resulting in more efficient PLEDs at higher voltage and luminance.

ACKNOWLEDGMENTS

[1]M. Kuik, G.-J. A. H. Wetzelaer, H. T. Nicolai, N. I. Crăciun, D. M. De Leeuw, and P. W. M. Blom, Adv. Mater. **26**, 512 (2014).
[2]H. T. Nicolai, M. Kuik, G. A. H. Wetzelaer, B. de Boer, C. Campbell, C. Risko, J. L. Brédas, and P. W. M. Blom, Nat. Mater. **11**, 882 (2012).
[3]P. W. M. Blom and M. J. M. de Jong, IEEE J. Sel. Top. Quantum Electron. **4**, 105 (1998).
[4]D. E. Markov and P. W. M. Blom, Phys. Rev. B. **72**, 161401(R) (2005).
[5]B. R. Lee, J. Kim, D. Kang, D. W. Lee, S.-J. Ko, H. J. Lee, C.-L. Lee, J. Y. Kim, H. S. Shin, and M. H. Song, ACS Nano **6**, 2984 (2012).
[6]J.-S. Kim, R. H. Friend, I. Grizzi, and J. H. Burroughes, Appl. Phys. Lett. **87**, 023506 (2005).
[7]K.-H. Yim, R. Friend, and J.-S. Kim, J. Chem. Phys. **124**, 184706 (2006).
[8]A. Köhnen, M. Irion, M. Gather, N. Rehmann, P. Zacharias, and K. Meerholz, J. Mater. Chem. **20**, 3301 (2010).
[9]H. T. Nicolai, A. Hof, J. L. M. Oosthoek, and P. W. M. Blom, Adv. Funct. Mater. **21**, 1505 (2011).
[10]D. Abbaszadeh, H. T. Nicolai, N. I. Crăciun, and P. W. M. Blom, Phys. Rev. B **90**, 205204 (2014).
[11]O. V. Mikhnenko, M. Kuik, J. Lin, N. van der Kaap, T.-Q. Nguyen, and P. W. M. Blom, Adv. Mater. **26**, 1912 (2014).
[12]N. Aizawa, Y.-J. Pu, H. Sasabe, and J. Kido, Org. Electron. **14**, 1614 (2013).
[13]N. Rehmann, D. Hertel, K. Meerholz, H. Becker, and S. Heun, Appl. Phys. Lett. **91**, 103507 (2007).
[14]S.-R. Tseng, H.-F. Meng, C.-H. Yeh, H.-C. Lai, S.-F. Horng, H.-H. Liao, C.-S. Hsu, and L.-C. Lin, Synth. Met. **158**, 130 (2008).
[15]G. Cheng, M. Mazzeo, S. Carallo, H. Wang, Y. Ma, and G. Gigli, Appl. Phys. Lett. **97**, 103107 (2010).
[16]T. Ye, S. Shao, J. Chen, L. Wang, and D. Ma, ACS Appl. Mater. Interfaces **3**, 410 (2011).
[17]Z. Liu, S. Tseng, Y. Chao, C.-Y. Chen, H. Meng, S.-F. Horng, Y.-H. Wu, and S.-H. Chen, Synth. Met. **161**, 426 (2011).
[18]M. Cai, T. Xiao, Y. Chen, E. Hellerich, R. Liu, R. Shinar, and J. Shinar, Appl. Phys. Lett. **99**, 203302 (2011).
[19]H. A. Al-attar and A. P. Monkman, J. Appl. Phys. **109**, 074516 (2011).
[20]N. I. Crăciun, J. Wildeman, and P. W. M. Blom, J. Phys. Chem. C **114**, 10559 (2010).
[21]C. Tanase, J. Wildeman, and P. W. M. Blom, Adv. Funct. Mater. **15**, 2011 (2005).
[22]See http://www.sigmaaldrich.com/catalog/product/aldrich/182605?lang=en&region=NL for energy levels (LUMO & HOMO) of PVK.
[23]M. C. Gather, F. Ventsch, and K. Meerholz, Adv. Mater. **20**, 1966 (2008).
[24]B. T. van Woudenbergh, J. Wildeman, P. W. M. Blom, J. J. A. M. Bastiaansen, and B. M. W. Langeveld-Vos, Adv. Funct. Mater. **14**, 677 (2004).